Unified model of fractal conductance fluctuations for diffusive and ballistic semiconductor devices

C. A. Marlow,[1] R. P. Taylor,[1,*] T. P. Martin,[1] B. C. Scannell,[1] H. Linke,[1] M. S. Fairbanks,[1] G. D. R. Hall,[1] I. Shorubalko,[2] L. Samuelson,[3] T. M. Fromhold,[4] C. V. Brown,[5] B. Hackens,[6] S. Faniel,[6] C. Gustin,[6] V. Bayot,[6] X. Wallart,[7] S. Bollaert,[7] and A. Cappy[7]

[1]*Materials Science Institute, Physics Department, University of Oregon, Eugene, Oregon 97403-1274, USA*

[2]*Institute of Solid State Physics, University of Latvia, Kengarga 8, LV-1063, Riga, Latvia*

[3]*Solid State Physics and The Nanometer Consortium, Lund University, Box 118, S-221 00 Lund, Sweden*

[4]*School of Physics and Astronomy, University of Nottingham, N11 8NS, United Kingdom*

[5]*School of Biomedical and Natural Sciences, Nottingham Trent University, NG7 2RD, United Kingdom*

[6]*CERMIN, PCPM, and DICE Labs, Université Catholique de Louvain, B-1348, Belgium*

[7]*IEMN, Cité Scientifique, Villeneuve d'Ascq, France*

(Received 20 September 2005; published 19 May 2006)

We present an experimental comparison of magnetoconductance fluctuations measured in the ballistic, quasiballistic, and diffusive scattering regimes of semiconductor devices. In contradiction to expectations, we show that the spectral content of the magnetoconductance fluctuations exhibits an *identical* fractal behavior for these scattering regimes and that this behavior is remarkably insensitive to device boundary properties. We propose a unified model of fractal conductance fluctuations in the ballistic, quasiballistic, and diffusive transport regimes, in which the generic fractal behavior is generated by a subtle interplay between boundary and material-induced chaotic scattering events.

DOI: 10.1103/PhysRevB.73.195318 PACS number(s): 75.47.Jn, 73.23.−b, 73.21.Hb, 73.21.La

I. INTRODUCTION

Ballistic electron devices represent a remarkable achievement of semiconductor growth and fabrication technology.[1–4] According to the traditional definition of ballistic transport, the electron's mean free path l (specifically, the momentum relaxation length extracted from electron mobility measurements) is sufficiently large that it satisfies the condition $l > (W,L)$, where W and L are the width and length of the device's conducting channel.[1] This contrasts with the more conventional quasiballistic[1] and diffusive[1] devices, defined, respectively, by the conditions $W < l < L$ and $l < (W,L)$. By reducing material-induced scattering events, a diverse range of experiments performed on ballistic devices have successfully demonstrated electron conduction processes that are dominated and controlled by the properties of the device boundaries.[1–3] The traditional system for these studies is the two-dimensional electron gas (2DEG) which forms at the interface of a semiconductor heterostructure[1–11] [Figs. 1(a) and 1(b)]. When the planar surface of the 2DEG is enclosed by boundary walls, the resulting device is commonly referred to as a "billiard" because of its appealing analogy to a billiard table. This ability to fabricate billiards relies on the "modulation doping" technique shown in Figs. 1(a) and 1(b). Ionized donors are separated spatially from the 2DEG plane in order to minimize any perturbations in the electrostatic potential landscape of the billiard.[1] Consequently, the donors only scatter the electrons through small angles and the associated deviations in the trajectories are not sufficient to reduce l to below the billiard dimensions. Therefore, despite featuring material-induced disorder, transport through these devices is referred to as ballistic and we adopt this standard nomenclature in this paper.

According to groundbreaking studies, the key properties of the billiard boundaries—"softness" (the gradient of the confining potential) and "geometry" (the shape enclosed by the potential)—dictate whether the electron dynamics is stable, chaotic, or mixed stable, and chaotic.[5,7–10] Crucially, this picture assumes that small-angle scattering from the donors does not strongly influence the electron dynamics and "real" semiconductor billiards are expected to display the same dynamical behavior as "idealized" billiards where material-induced disorder is completely absent. However, recent scanning probe measurements,[11,12] used to map the spatial distribution of electrons in ballistic devices, have rekindled interest in the precise role of these material-induced scattering events. These measurements show that the ionized donors induce remarkably intricate deviations from straight trajectories.[12] Although the donors do not backscatter the electrons, the spatial complexity traced out by the trajectories raises the question of how this disorder impacts conduction properties that are sensitive to the *precise* form of the electron dynamics. Is the billiard's dynamical form (chaotic, stable or mixed) immune to the presence of material-induced small-angle scattering as previously suggested,[5,7–9] or does this scattering play a central role in establishing a form of dynamics shared with strongly disordered systems, in particular that generated by the large-angle scattering events that dominate diffusive conduction?

In this paper, we address this question by using low-temperature measurements of magnetoconductance fluctuations as a sensitive probe of the electron dynamics. In contrast to classical processes, the quantum interference processes that generate the magnetoconductance fluctuations are *critically* sensitive to the *precise* spatial configuration of scatterers. In particular, spectral analysis of the fluctuations has served as a powerful method for investigating electron scattering dynamics.[9,13] Here, we present a comprehensive experimental comparison of magnetoconductance fluctua-

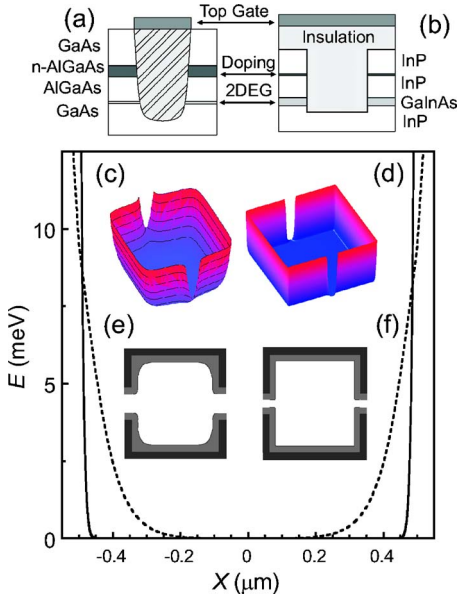

FIG. 1. (Color online) Schematic representations of the two billiard systems and simulations of their confinement potentials. (a) For the GaAs/AlGaAs billiards, a negative voltage applied to a patterned top gate is used to electrostatically deplete a corresponding pattern (indicated by the striped region) in the 2DEG to form the billiard boundary. (b) For the GaInAs/InP billiards, the billiard boundary is formed by an etching down through the 2DEG. A uniform top gate, deposited above an insulation layer (gray region), is used to reduce the Fermi energy and hence the number of populated modes in the quantum point contact (QPC) leads (Refs. 1 and 15). The dopant-2DEG separations are 15 nm and 20 nm and the gate-2DEG separations are 90 nm and 1 μm in (a) and (b), respectively. (c), (d) Simulations of the potential energy profile in the plane of the 2DEG for (c) a GaAs/AlGaAs billiard (device *c* of Ref. 11) and (d) the GaInAs/InP billiard *b*. (e), (f) Top views of the resulting geometries (gray indicates the depletion region in the 2DEG). Main figure: a cross section of the potential energy E vs spatial location X across the billiard's central region. The dashed and bold lines are for the GaAs/AlGaAs and GaInAs/InP billiards respectively.

tions measured on 30 devices spanning the ballistic, quasiballistic, and diffusive scattering regimes. We show that the spectral content of the magnetoconductance fluctuations exhibits an *identical* fractal behavior in the three scattering regimes and that this behavior is remarkably insensitive to device boundary properties.

We propose a model of fractal conductance fluctuations (FCF's) that unifies the three scattering regimes. Although modulation doping reduces material-induced scattering and ensures $l > (W,L)$ for ballistic systems, we propose that the role of small-angle scatterers in the electron interference processes that generate the fractal conductance fluctuations is enhanced by multiple traversals within the system. Consequently, for all three scattering regimes, material-induced chaotic scattering generates the observed generic fractal behavior in the spatial electron wave patterns[11] and in the resulting FCF spectra. This fractal process is, however, suppressed for classical and quantum conduction effects generated by relatively short trajectories that do not encounter many scatterers, allowing geometry-induced effects to dominate. Although our model is therefore consistent with many previously observed geometry-induced ballistic effects,[1] it is currently unclear how our experiments relate to other studies of magnetoconductance fluctuations that are described purely in terms of boundary-induced processes.[9,14] The investigations presented in this paper therefore emphasize that the effect of material-induced disorder on electron interference is not fully understood and that further experimental and theoretical investigations are needed.

II. EXPERIMENT

We begin by investigating the role of the billiard boundaries and compare billiards with varying degrees of boundary softness and a wide range of geometries. To do this, we use both conventional GaAs/AlGaAs heterostructures, in which patterned top gates define the billiard boundaries [Fig. 1(a)] and a GaInAs/InP heterostructure system in which the boundaries are defined by wet etching [Fig. 1(b)].[15] For the GaInAs/InP billiards, a uniform top gate, deposited above an insulation layer [see Fig. 1(b)], is used to reduce the Fermi energy E_F.[1,15] The experimental parameters for the 16 GaInAs billiards (labeled $a-p$) are listed in Table I, and those of the 9 GaAs/AlGaAs billiards are described in our previous studies.[4,6] We emphasize that both material systems are characterized by l values that are typical of ballistic experiments[1] and that the 25 billiards considered satisfy the ballistic condition $l > (W,L)$. The solid curve in Fig. 1 shows an experimentally confirmed simulation of the potential energy profile for an electron in billiard *b*,[15] while the dashed curve shows the simulated profile of a surface-gated GaAs/AlGaAsbilliard.[6] To quantify the profile "softness," P, we use the potential energy gradient at E_F.[6] The P value of the GaInAs/InP billiards is an order of magnitude steeper than for the GaAs/AlGaAs billiard (at $E_F = 10$ meV the respective P values are 1.29 meV/nm and 0.17 meV/nm). The steeper profile results mainly from the close proximity of the surface charge on the etched boundary to the 2DEG compared to the more remote patterned top gates of the AlGaAs/GaAs billiards.[15]

Each billiard features two quantum-point contacts (QPC's) that form the entrance and exit ports for conduction through the billiard's enclosed cavity. Trace (a) of Fig. 2 shows the conductance, G, measured at temperature $T = 4.2$ K and plotted against gate bias V_g for a single QPC fabricated in the GaInAs/InP 2DEG. The conductance plateaus observed at integer values of $2e^2/h$ (where e is the electronic charge and h is Planck's constant) are well-established signatures of ballistic transport.[1,16] Trace (b) of Fig. 2 shows G measured at $T = 4.2$ K and plotted against V_g for billiard *c*. Compared to the single QPC, the billiard's plateaus occur at much lower conductance values. The integer steps of e^2/h indicate that electron trajectories interact significantly with the billiard's central cavity, reducing the device conductance due to the addition of the two QPC resistances.[17] As the billiard is cooled to lower temperatures, electron-wave interference contributes to the cavity's transmission properties and reproducible fluctuations emerge superimposed on the plateaus [see, for example, trace (c) which is measured at $T = 240$ mK].

TABLE I. Details of the billiards ($a-p$) and wires ($q-u$). Scanning electron micrographs of the GaInAs billiards a and $f-p$ ($b-e$ have identical geometries to a) and a summary of their experimental parameters: l, the mean free path (determined from mobility measurements); L and W, the device lithographic length and width; A, the billiard's enclosed area determined from the profile measurements (Ref. 15) note that for the wires $q-u$, the analogous area is the "phase-coherent subregion" (Ref. 34 enclosed by a rectangle with side lengths given by the minimum of the phase coherence length and the device dimension); n, the number of populated QPC modes; T, temperature; τ_q, the electron phase-coherence time (measured using a correlation analysis) (Ref. 35), and Q. Billiards $l-p$ are defined in a GaInAs/InAlAs heterostructure, in which InAlAs assumes an analogous role to InP in GaInAs/InP billiards (Ref. 36)

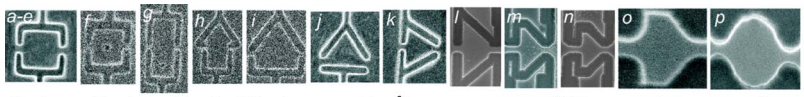

Device	l(μm)	L(μm) x W(μm)	A (μm^2)	n	T (K)	τ_q(ps)	Q
a	4.7-5.4	0.96 x 0.93	0.63-0.77	1-8	0.24-6.0	2-100	0.72-0.016
b	6.0-6.2	0.96 x 0.93	0.65-0.89	1-5	0.24-7.0	0.6-32	0.58-0.023
c	5.9-6.1	0.96 x 0.93	0.63-0.77	1-8	0.24	19-36	0.60-0.35
d	5.2	0.42 x 0.42	0.12-0.13	8-9	0.24	58-61	7.5-7.4
e	3.2-3.6	0.75 x 0.75	0.16-0.2	1-4	0.24	19-48	3.8-2.0
f	2.9-3.7	0.94 x 1.1	0.35-0.46	1-5	0.24-6.5	12-30	0.86-0.040
g	2.9-3.7	0.90 x 1.9	0.95-0.98	3-7	0.24-6.5	15-35	0.56-0.019
h	3.1-3.9	0.93 x 0.82	0.73-0.75	3-12	0.24-6.0	22-67	0.52-0.026
i	3.1-3.9	1.4 x 0.6	0.73-0.81	2-6	0.24-6.0	20-35	0.50-0.025
j	6.1-6.2	1.2 x 1.2	0.42-0.49	1-6	0.24	10-24	0.69-0.31
k	6.1-6.2	0.84 x 1.1	0.43-0.50	1-7	0.24	7-47	0.97-0.23
l	1.8	0.63 x 1.3	0.28	5	0.4-15.3	5-28	1.7-0.031
m	1.8	0.48 x 0.79	0.13	5	0.4-15.3	0.4-23	3.4-0.078
n	1.8	0.38 x 0.62	0.09	2	0.4-15.3	0.1-14	2.8-0.11
o	0.50	0.46 x 0.43	0.13	8	0.3-11.7	19-50	6.6-0.087
p	0.50	0.48 x 0.57	0.11	3	1.3-24.0	1-11	0.90-0.050
q	0.97	30 x 0.55	2.2	-	0.04-4.0	125	0.51 - 0.010
r	0.36	3.5 x 0.96	0.56 - 0.59	-	1.4	7	0.20 -0.19
s	0.041	1.3 x 0.60	0.0072 - 0.0086	-	4.2-50.0	0.1-0.5	0.16 - 0.06
t	0.030	10 x 0.26	0.0039 - 0.0059	-	4.2-37.5	0.2-0.3	0.50 - 0.35
u	0.050	2.0 x 0.30	0.040 -0.097	-	1.5 - 4.2	2-6	0.37 - 0.33

To investigate the degree to which this transmission is determined by the cavity's boundary properties, we compare transport through the "soft" GaAs/AlGaAs billiards and the "harder" GaInAs/InP billiards. We adopt the common experimental strategy of investigating the quantum fluctuations as a function of magnetic field B applied perpendicular to the plane of billiard rather than as a function of V_g. Whereas B and V_g both generate conductance fluctuations by changing the phase of the electron waves, using a magnetic field as the experimental variable has the considerable advantage of not changing other crucial billiard properties such as E_F and P. We build on investigations showing that the magnetoconductance fluctuations have a fractal spectral content,[4,6,7,11] and use this generic property as a characterization tool. The black curve in the inset of Fig. 3(a) shows G measured at $T=0.6$ K on billiard b and plotted against B. According to the Aharonov-Bohm[1] model for quantum interference of electron waves traveling along the classical trajectories, the equation $f=eA_t/h$ (where $f=1/\Delta B$) can be used to relate the frequency spectrum of the conductance fluctuations to the distribution of areas A_t enclosed by these trajectories.[9,13] Analysis of the fluctuations' power spectrum $S(f)$ therefore provides an intuitive probe of the electron trajectory distributions.[9,13] In Fig. 3(a) we show that $S(f)$ follows a $1/f^{\alpha}$ behavior. This power law is consistent with fractal scaling[18] in the $G(B)$ curves, and the spectral scaling exponent α can be related to the fractal dimension D (the scaling parameter commonly used in fractal studies) by the established relationship $\alpha=(5-2D)$.[18] The traditional "box-counting" fractal analysis of $G(B)$, employed to obtain D directly,[4,7] is shown in Fig. 3(b). This fractal scaling behavior occurs over a significantly larger scaling range than for typical observations of physical fractals.[19]

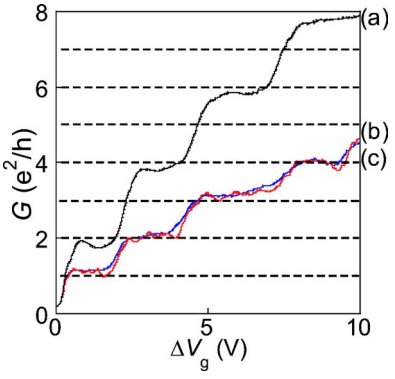

FIG. 2. (Color online) Conductance G plotted against gate bias ΔVg (the bias measured relative to the voltage required to form the QPC's first mode) for (a) a single QPC measured at $T=4.2$ K (black line), (b) billiard c measured at $T=4.2$ K (bold blue line), and (c) billiard c measured at $T=240$ mK (fine red line). All QPC's have lithographic dimensions of 0.1 μm by 0.2 μm.

Consistent with our previous measurements of GaAs/AlGaAs billiards,[4] we find that the α values of the FCF measured on GaInAs/InP billiards depend solely on the empirically determined parameter Q, which is the ratio of the

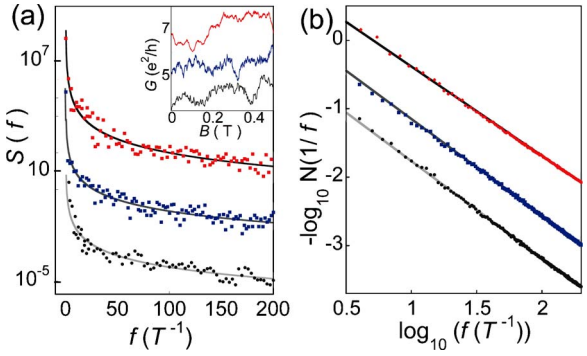

FIG. 3. (Color online) Magnetoconductance fluctuation traces and their fractal analysis for a billiard and a quasiballistic wire, together with a simulated fractal trace which is included for comparison with the experimental data. Inset of (a): the magnetoconductance fluctuations of the quasiballistic wire q at $T=0.5$ K (red), a simulated fractal trace (blue), and the magnetoconductance fluctuations of billiard b at $T=0.6$ K (black). (a) The power spectra, S vs f, of the three traces in the inset, along with best-fit curves. (b) The box-counting fractal analysis, where the number $N(\Delta B)$ of squares required to cover the $G(B)$ trace scales according to $N(\Delta B) \sim \Delta B^{-D}$ (the box size ΔB is related to f by $f=1/\Delta B$). The $S(f)$ spectrum exhibits more data scatter than the box-counting technique, as expected (Ref. 33). The associated α values are (top to bottom) 2.4, 2.2, and 2.2, respectively. All traces are offset vertically for clarity.

billiard's average energy-level spacing ΔE_s to the average energy-level broadening ΔE_B:

$$Q = \frac{\Delta E_s}{\Delta E_B} = \frac{(2\pi\hbar^2)/(m^* A)}{\sqrt{(\hbar/\tau_q)^2 + (kT)^2}}, \tag{1}$$

where m^* is the electronic effective mass, A is the billiard's enclosed area, and τ_q is the electron phase coherence time. In Fig. 4(a), 67 values of α measured for 5 square GaInAs/InP billiards are plotted as a function of Q (blue squares). As a demonstration of this evolution of α with Q, in Fig. 5(a) we show some of the FCF traces that produce the sharp drop in α below $Q=1$. As T is decreased, the induced increase in τ_q [shown in the inset of Fig. 5(a)] produces a rise in Q. This is accompanied by an increase in high-frequency fluctuations observed in the FCF in Fig. 5(a) and leads to the drop in α plotted in the inset of Fig. 5(a).

The α values in Fig. 4(a) are measured on billiards *a–e* for a range of values of A, T, τ_q, and n, the number of conducting modes in the QPC's, and demonstrate that all of the α data lie on a single "Q curve." This distinct evolution of α, charted across a wide range of billiard conditions, provides a technique for gauging the relative impact of wall *softness* on the spectral signature of the FCF's, as we now explain. To investigate the dependence of α on boundary softness, we also plot 49 α values measured on 9 GaAs/AlGaAs billiards[4] in Fig. 4(a). The data show that, despite the softer wall profile of these billiards, they follow the *same* Q curve as the harder GaInAs/InP billiards. Any variation in α between the soft and hard billiards lies well within experimental uncertainty and is substantially smaller than the differences in α induced by changes in Q. Therefore, in contrast to

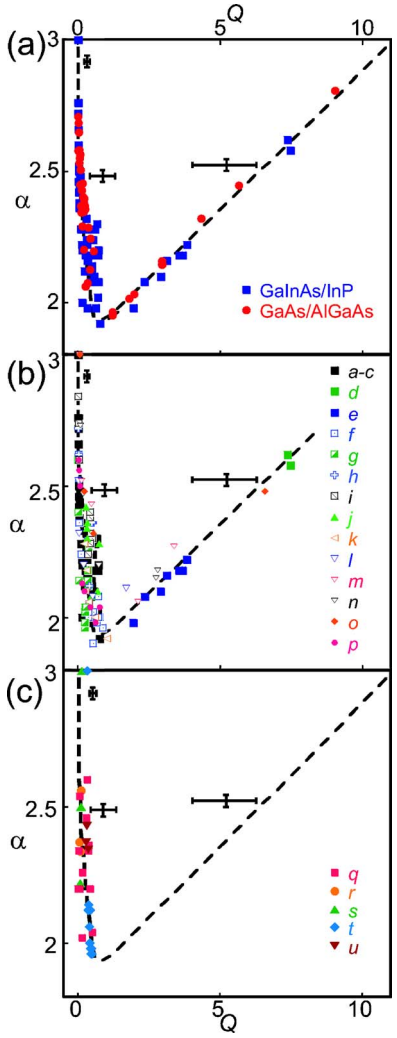

FIG. 4. (Color online) Q curves for the devices. (a) α plotted against Q for soft-walled GaAs/AlGaAs and harder-walled GaInAs/InP (billiards *a–e*) square-shaped billiards. (b) α plotted against Q for the different shaped GaInAs billiards (billiards *a–p*). (c) α plotted against Q for a quasiballistic wire q and diffusive wires *r–u*. The dashed line, which is identical for all three plots, is a guide to the eye. Measurement uncertainties vary in magnitude across the "Q curve" as indicated by the error bars.

theoretical predictions, the FCF spectral content does *not* depend critically on the exact form of the potential.[5]

To investigate the dependence of α on billiard *geometry*, we exploit the superior shape fidelity provided by our harder-walled GaInAs billiards and compare α values measured for the diverse range of geometries shown in Table I. In contrast to expectations,[8,9] Fig. 4(b) reveals that α does *not* depend on geometry either: the 94 α values for devices *f–p* lie, within experimental scatter, on the *same* Q curve as the square billiards. An intriguing explanation for this insensitivity to both boundary shape and softness is that material-induced scattering plays a much more important role than previously assumed for FCF's. This speculation is further supported by thermally cycling the billiards. Our measurements show that thermal cycling does not affect the billiard geometry or the steepness of the long-range smooth potential

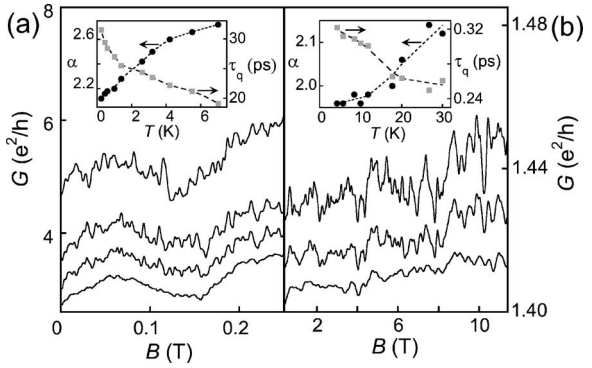

FIG. 5. Magnetoconductance fluctuation traces and associated analysis for a billiard and a diffusive wire. (a) Magnetoconductance fluctuations measured on billiard b for $n=4$. The top trace is measured at $T=0.24$ K ($Q=0.50$) before thermal cycling to $T=295$ K. The remaining traces are measured after thermal cycling, at (top to bottom) $T=0.24$ K ($Q=0.50$), 1.4 K ($Q=0.12$), and 7.0 K ($Q=0.023$). Traces in (a) and (b) are vertically offset for clarity. The inset to (a) shows α (black circles) and τ_q (gray squares) plotted against T for $n=4$. (b) Magnetoconductance fluctuations measured on a diffusive n^+-GaAs wire (Ref. 13) r at (top to bottom) $T=4.2$ K ($Q=0.50$), 11.8 K ($Q=0.47$), and 30.0 K ($Q=0.38$). The inset to (b) shows α (black circles) and τ_q (gray squares) plotted against T. Traces in (a) and (b) are vertically offset for clarity.

profile (i.e., the profile softness). However, thermal cycling is known to redistribute charge among the dopants,[20] producing local changes in the potential landscape. The modified spatial distribution of dopant scattering sites induces major changes in the details of the fluctuations: compare, for example, the top two traces of Fig. 5(a), which are measured on billiard b at $T=240$ mK before and after thermal cycling to $T=295$ K. Significantly, the α value of the fluctuation spectrum is robust to these changes in the individual fluctuations.

III. DISCUSSION

We propose the following explanation for FCF's which explains the key experimental observations. Ionized donors and residual carbon dopants create small perturbations[21] superimposed on the smooth, boundary-induced potential profiles of Fig. 1. The resulting roughness in the potential landscape, which is of the order of several meV (an order of magnitude smaller than E_F),[21] induces a chaotic scattering of trajectories as the electrons traverse the billiard. The role of the boundaries is simply to amplify the effect of these small-angle scatterers so that even ballistic devices act as disordered systems for the electron-wave interference processes that generate the FCF's. This is achieved through multiple reflections from the boundaries that send the trajectories and corresponding electron waves repeatedly through the rough potential landscape. For both billiard systems, electrons undergo up to 50 traversals of the billiard before dephasing. This iteration of chaotic dynamics is common to many fractal processes[18] and generates complexity in the trajectory distribution on many spatial scales. Due to flux cancellation effects,[1] the Aharonov-Bohm relation $f=eA_t/h$ is sensitive to the *net* area enclosed by these trajectories, explaining why the observed lower-frequency cut off of fractal behavior corresponds to areas up to 5 times smaller than that of the billiard (see Ref. 6 and Fig. 3).

This proposed origin of FCF's is consistent with the recent scanning probe measurements of electrons emerging from a QPC.[12] The intricate deviations from straight trajectories, which were explained in terms of scattering induced by ionized donors, bear a striking resemblance to the branching pattern of a fractal tree.[18] In our picture, boundary reflections cause this branching process to repeat, with each traversal of the billiard inducing more complex interference and branching flow patterns in the electron waves. Indeed, recent scanning probe measurements confirm that the spatial distribution of electron waves in a billiard is fractal.[11] Since the role of the boundaries in the formation of this fractal distribution is limited to reflecting the trajectories into the chaotic scatterers produced by the rough potential landscape, the fractal scaling properties will be insensitive to boundary softness and geometry, as observed in the measured FCF's of our billiards. Classical and quantum conduction effects generated by short trajectories, which leave the billiard without undergoing many traversals through the chaotic scatterers, will be determined predominantly by the billiard geometry.[22] This becomes more apparent for "open" geometries where the trajectories undergo few traversals of the device. Such geometries include QPC's,[1,2] Hall junctions,[23] Maltese crosses,[1] and electrostatic lenses[24] and for small billiards where the entrance and exit widths occupy a relatively large section of the billiard boundary.

This picture predicts that magnetoconductance fluctuations measured on wires in the quasiballistic[1] and diffusive[1] regimes should also be fractal. Fractal fluctuations have previously been measured on a quasiballistic Au wire.[25] However, this was interpreted subsequently in terms of a fortuitous narrowing of the wire that created a ballistic cavity rather than due to quasiballistic scattering.[7] Our analysis of a quasiballistic GaAs/AlGaAs wire[26] (see wire q in Table I) confirms that the conductance fluctuations of quasi-ballistic systems have the *same* fractal scaling behavior as the billiards. An example FCF trace and the corresponding analysis are shown in Fig. 3 (red curve) and Fig. 5(b). Furthermore, we investigate four diffusive wires made from GaAs/AlGaAs (Ref. 27) (wires r and s) and n^+-GaAs (Refs. 13 and 28) (wires t and u) and show that FCF behavior extends to the diffusive transport regime. Significantly, the n^+-GaAs wires do not feature the modulation doping technique—the donors are located in the conducting plane of the wire, generating large-angle scattering events. Again, despite this difference in the level of material-induced disorder, the FCF's follow the same behavior as the billiards: the α values from 36 FCF traces measured for the quasiballistic and diffusive devices are mapped onto the Q curve in Fig. 4(c), demonstrating that the FCF's follow the same Q curve for all three scattering regimes. We reemphasize the role of the billiard boundaries in this observed unification of FCF—although the large-angle scatterers of the diffusive material produce much smaller mean free paths than the small-angle scatterers of ballistic material, the iterative traversal process across the billiard ensures a similar level of spatial complexity in the trajectory patterns.

IV. CONCLUSIONS

It is well known that the small-angle scattering processes of ballistic devices can generate radically different conduction properties compared to the large-angle scattering processes of diffusive devices, ranging from enhanced electron mobility effects to conductance plateaus.[1] In this paper, we have shown that, despite the distinctly different degrees of material-induced disorder, these scattering regimes exhibit unexpected similarities in the form of electron dynamics. Spectral analysis of magnetoconductance fluctuations is a well-established method for investigating electron scattering dynamics in semiconductors. We have presented a comprehensive comparison of 9 soft-walled billiards, 16 hard-walled billiards, 1 quasiballistic device, and 4 diffusive devices and demonstrated that the spectral content of the fluctuations follows an identical fractal behavior across the diffusive, quasiballistic and ballistic scattering regimes. Previous theories of FCF's (Refs. 5 and 29) do not explain this unification.

In light of the diverse range of devices used in our experiments, it would be informative for future studies to examine the extent of this "universality" of fractal conductance fluctuations and to determine how our model of material-induced scattering relates to other studies where purely boundary-induced processes are used to explain magnetoconductance fluctuations.[9,14] In particular, it would be useful to reexamine the circle and stadium billiards used in the original geometry-dependence studies[9] to determine how the α values fit on the Q curve. Furthermore, we emphasize that the billiards used in our studies were fabricated from materials with mean free paths similar to those of typical previous billiard experiments. It would be of considerable interest to investigate whether FCF's persist in 2DEG *systems* where ionized donors are absent and the degree of material-induced disorder is therefore radically reduced.[30] We hope that these issues will motivate the development of a detailed theoretical model of fractal conductance fluctuations in semiconductor environments.[31,32] A particular challenge for future theoretical investigations concerns the role of Q in the quantum interference of the fractal electron wave pattern and how this determines the fractal scaling factor α of the FCF's and the form of the Q curve shown in Fig. 4.

Finally, the robustness of FCF's to variations in boundary properties and material-induced disorder indicates that FCF's might be far more prevalent than previously anticipated, appearing in the conductance of enclosed cavities fabricated by a wide range of techniques. Coupling this prevalence with the basic form of Q leads to the striking prediction that a variety of cavities might display fractal conductance fluctuations in their *room-temperature* operation [for example, using the material parameters of bismuth,[27] Eq. (1) predicts that a 50-nm cavity corresponds to $Q=1$ at $T=293$ K]. This result might hold important implications for nanodevice applications. Due to their inherent unpredictability and critical sensitivity to device parameters that vary the electron phase (such as gate potentials), FCF's may represent a fundamental limitation for the performance of future devices featuring nanoscale cavities. A greater understanding of the origin of FCF's is therefore important for fundamental and applied aspects of nanoscale physics.

ACKNOWLEDGMENTS

We thank A. P. Micolich for his help in the early stages of this project, J. P. Bird and K. Ishibashi for supplying MCF data from Refs. 24–26, and R. Haydock and J. Nöckel for valuable discussions. B.H. and S.F. are supported by FRIA and the EC.

*Corresponding author. Electronic address: rpt@uoregon.edu

[1] C. W. J. Beenakker and H. van Houten, *in Solid State Physics*, edited by H. Ehrenreich and D. Turnbull (Academic Press, Boston, 1991), Vol. 44.

[2] K.-F. Berggren and M. Pepper, Phys. World **15**, 37 (2002).

[3] J. H. Davies, *The Physics of Low Dimensional Structures: An Introduction* (Cambridge University Press, New York, 1998); J. P. Bird, *Electron Transport in Quantum Dots* (Kluwer Academic, New York, 2003).

[4] A. P. Micolich, R. P. Taylor, A. G. Davies, J. P. Bird, R. Newbury, T. M. Fromhold, A. Ehlert, H. Linke, L. D. Macks, W. R. Tribe, E. H. Linfield, D. A. Ritchie, J. Cooper, Y. Aoyagi, and P. B. Wilkinson, Phys. Rev. Lett. **87**, 036802 (2001).

[5] R. Ketzmerick, Phys. Rev. B **54**, 10841 (1996).

[6] R. P. Taylor, R. Newbury, A. P. Micolich, T. M. Fromhold, H. Linke, A. G. Davies, T. P. Martin, and C. A. Marlow, in *Electron Transport in Quantum Dots*, edited by J. P. Bird (Kluwer Academic/Plenum, New York, 2003).

[7] A. S. Sachrajda, R. Ketzmerick, C. Gould, Y. Feng, P. J. Kelly, A. Delage, and Z. Wasilewski, Phys. Rev. Lett. **80**, 1948 (1998).

[8] R. A. Jalabert, H. U. Baranger, and A. D. Stone, Phys. Rev. Lett. **65**, 2442 (1990).

[9] C. M. Marcus, A. J. Rimberg, R. M. Westervelt, P. F. Hopkins, and A. C. Gossard, Phys. Rev. Lett. **69**, 506 (1992).

[10] R. P. Taylor, R. Newbury, A. S. Sachrajda, Y. Feng, P. T. Coleridge, C. Dettmann, N. Zhu, H. Guo, A. Delage, P. J. Kelly, and Z. Wasilewski, Phys. Rev. Lett. **78**, 1952 (1997).

[11] R. Crook, C. G. Smith, A. C. Graham, I. Farrer, H. E. Beere, and D. A. Ritchie, Phys. Rev. Lett. **91**, 246803 (2003).

[12] M. A. Topinka, B. J. LeRoy, R. M. Westervelt, S. E. J. Shaw, R. Fleischmann, E. J. Heller, K. D. Maranowski, and A. C. Gossard, Nature (London), **410**, 183 (2001).

[13] R. P. Taylor, M. L. Leadbeater, G. P. Whittington, P. C. Main, L. Eaves, S. P. Beaumont, I. McIntyre, S. Thoms, and C. D. W. Wilkinson, Surf. Sci. **196**, 52 (1988).

[14] J. P. Bird, A. P. Micolich, H. Linke, D. K. Ferry, R. Akis, Y. Ochiai, Y. Aoyagi, and T. Sugano, J. Phys.: Condens. Matter **10**, L55 (1998).

[15] T. P. Martin, R. P. Taylor, H. Linke, C. A. Marlow, G. D. R. Hall, I. Shorubalko, I. Maximov, W. Seifert, L. Samuelson, and T. M. Fromhold, Superlattices Microstruct. **34**, 179 (2003).

[16] Generated by the depopulation of the QPC's one-dimensional conduction modes as E_F is reduced by the gate bias, the plateaus have broader steps than expected for idealized, disorder-free QPC's. This broadening, which is a standard characteristic of real QPC's, is attributed to the presence of the ionized donors (Ref. 31).

[17] If the trajectories were unhindered by the cavity, the device conductance plateaus would occur at the integer values of $2e^2/h$ (Ref. 32) .

[18] M. F. Barnsley, R. L. Devaney, B. B. Mandelbrot, H.-O. Peitgen, D. Saupe, and V. R. F. w. c. b. Y. F. a. M. Mcguire, *The Science of Fractal Images* (Springer-Verlag, New York, 1988).

[19] D. Avnir, O. Biham, D. A. Lidar, and O. Malcai, Science **279**, 39 (1998).

[20] R. P. Taylor, P. C. Main, L. Eaves, S. P. Beaumont, S. Thoms, and C. D. W. Wilkinson, in *ICPS-19* (Polish Academy of Sciences, Warsaw, 1988), 1, 83.

[21] J. A. Nixon and J. H. Davies, Phys. Rev. B **41**,7929 (1990).

[22] L. Christensson, H. Linke, P. Omling, P. E. Lindelof, I. V. Zozoulenko, and K.-F. Berggren, Phys. Rev. B **57**, 12306 (1998); J. P. Bird, D. K. Ferry, R. Akis, Y. Ochiai, K. Ishibashi, Y. Aoyagi, and T. Sugano, Europhys. Lett. **35**, 529 (1996); J. P. Bird, R. Akis, D. K. Ferry, D. Vasileska, J. Cooper, Y. Aoyagi, and T. Sugano, Phys. Rev. Lett. **82**, 4691 (1999).

[23] C. J. B. Ford, S. Washburn, M. Büttiker, C. M. Knoedler, and J. M. Hong, Phys. Rev. Lett. **62**, 2724 (1989).

[24] J. Spector, H. L. Stormer, K. W. Baldwin, L. N. Pfeiffer, and K. W. West, Appl. Phys. Lett. **56**, 1290 (1990).

[25] H. Hegger, B. Huckestein, K. Hecker, M. Janssen, A. Freimuth, G. Reckziegel, and R. Tuzinski, Phys. Rev. Lett. **77**, 3885 (1996).

[26] J. P. Bird, K. Ishibashi, Y. Ochiai, M. Lakrimi, A. D. C. Grassie, K. M. Hutchings, Y. Aoyagi, and T. Sugano, Phys. Rev. B **52**, 1793 (1995).

[27] K. Ishibashi, Y. Takagaki, K. Gamo, S. Namba, S. Takaoka, K. Murase, S. Ishida, and Y. Aoyagi, J. Vac. Sci. Technol. B **6**, 1952 (1988).

[28] K. Ishibashi, K. Nagata, K. Gamo, and S. Namba, Solid State Commun. **61**, 385 (1987).

[29] G. Benenti, G. Casati, I. Guarneri, and M. Terraneo, Phys. Rev. Lett. **87**, 014101 (2001); A. Budiyono and K. Nakamura, Chaos, Solitons Fractals **17**, 89 (2003); I. Guarneri and M. Terraneo, Phys. Rev. E **65**, 015203(R) (2001); E. Louis and J. A. Vergés, Phys. Rev. B **61**, 13014 (2000).

[30] B. E. Kane, G. R. Facer, A. S. Dzurak, N. E. Lumpkin, R. G. Clarke, L. N. Pfeiffer, and K. W. West, Appl. Phys. Lett. **72**, 3506 (1998).

[31] J. A. Nixon, J. H. Davies, and H. U. Baranger, Phys. Rev. B **43**, 12638 (1991).

[32] D. A. Wharam, M. Pepper, H. Ahmed, J. E. F. Frost, D. G. Hasko, D. C. Peacock, D. A. Ritchie, and G. A. C. Jones, J. Phys. C **21**, L887 (1988).

[33] B. Dubuc, J. F. Quiniou, C. Roques-Carmes, C. Tricot, and S. W. Zucker, Phys. Rev. A **39**, 1500 (1989).

[34] P. A. Lee, A. D. Stone, and H. Fukuyama, Phys. Rev. B **35**, 1039 (1987).

[35] J. P. Bird, K. Ishibashi, D. K. Ferry, R. Newbury, D. M. Olantana, Y. Ochiai, Y. Aoyagi, and T. Sugano, Surf. Sci. **361/362**, 730 (1996).

[36] B. Hackens, F. Delfosse, S. Faniel, C. Gustin, H. Boutry, X. Wallart, S. Bollaert, A. Cappy, and V. Bayot, Phys. Rev. B **66**, 241305(R) (2002).